Validation and Extension to Three Dimensions of the Berenger PML Absorbing Boundary Condition for FD-TD Meshes

Daniel S. Katz, *Fellow, IEEE*, Eric T. Thiele, *Student Member, IEEE*, and Allen Taflove, *Fellow, IEEE*

***Abstract*— Berenger recently published a novel absorbing boundary condition (ABC) for FD-TD meshes in two dimensions, claiming orders-of-magnitude improved performance relative to any earlier technique. This approach, which he calls the "perfectly matched layer (PML) for the absorption of electromagnetic waves," creates a nonphysical absorber adjacent to the outer grid boundary that has a wave impedance independent of the angle of incidence and frequency of outgoing scattered waves.**

This paper verifies Berenger's strong claims for PML for 2-D FD-TD grids and extends and verifies PML for 3-D FD-TD grids. Indeed, PML is > 40 dB more accurate than second-order Mur, and PML works just as well in 3-D as it does in 2-D. It should have a major impact upon the entire FD-TD modeling community, leading to new possibilities for high-accuracy simulations especially for low-observable aerospace targets.

I. Introduction

OVER THE past ten years, finite-difference time-domain (FD-TD) solutions of Maxwell's equations have been extensively applied to model open-region electromagnetic wave scattering problems. Here, a primary challenge has been in the area of absorbing boundary conditions (ABC's) at the outer grid boundaries. Existing analytical ABC's, such as Mur [1] and Liao [2], provide effective reflection coefficients in the order of -35 to -45 dB for most FD-TD simulations. To attain a dynamic range of 70 dB, comparable to that of current RCS measurement technology, 40 dB more accurate ABC's are needed than currently exist.

Such an advance appears to be at hand with the recent publication of Berenger's "perfectly matched layer (PML) for the absorption of electromagnetic waves [3]." PML involves creation of a nonphysical absorber adjacent to the outer grid boundary that has a wave impedance independent of the angle of incidence and frequency of outgoing scattered waves. In 2-D, Berenger reported reflection coefficients for PML as low as 1/3000th those of standard second- and third-order analytical ABC's such as Mur.

In this letter, we confirm these remarkable claims and then extend and verify PML for 3-D Cartesian FD-TD grids. Section II briefly summarizes key elements of Berenger's published 2-D PML theory [3]. Sections III and IV report our contributions, specifically the extension of PML to 3-D and the confirmation of the approach in 2-D and 3-D.

Manuscript received April 13, 1994. This work was supported in part by NSF Grant ECS-9218494, ONR Contract N00014-93-0133, and Cray Research Inc.

D. S. Katz is with Cray Research, Inc., El Segundo, CA 90245 USA.

E. T. Thiele and A. Taflove are with the EECS Department, McCormick School of Engineering, Northwestern University, Evanston, IL 60208 USA.

IEEE Log Number 9403322.

II. Two-dimensional TE Case [3]

Consider Maxwell's equations in 2-D for the transverse electric (TE) case with field components E_x, E_y, and H_z. If σ and σ^* denote electric conductivity and magnetic loss assigned to an outer boundary layer to absorb outgoing waves, respectively, it is well known that:

$$\sigma/\varepsilon_o = \sigma^*/\mu_o \tag{1}$$

provides for reflectionless transmission of a plane wave propagating normally across the interface between free space and the outer boundary layer. Layers of this type have been used in the past to terminate FD-TD grids [4]. However, the absorption is thought at best to be in the order of the analytical ABC's because of increasing reflection at oblique incident angles.

The PML technique introduces a new degree of freedom in specifying loss and impedance matching by splitting H_z into two sub-components, H_{zx} and H_{zy}. Here, there are four (rather than the usual three) coupled field equations:

$$\varepsilon_o \frac{\partial E_x}{\partial t} + \sigma_y E_x = \frac{\partial (H_{zx} + H_{zy})}{\partial y} \tag{2a}$$

$$\varepsilon_o \frac{\partial E_y}{\partial t} + \sigma_x E_y = -\frac{\partial (H_{zx} + H_{zy})}{\partial x} \tag{2b}$$

$$\mu_o \frac{\partial H_{zx}}{\partial t} + \sigma_x^* H_{zx} = -\frac{\partial E_y}{\partial x} \tag{3a}$$

$$\mu_o \frac{\partial H_{zy}}{\partial t} + \sigma_y^* H_{zy} = \frac{\partial E_x}{\partial y} \tag{3b}$$

Note that the TM case is obtained by duality, with E_z split into E_{zx} and E_{zy}. Designating ψ as any component of a wave propagating in a PML medium, Berenger shows that:

$$\psi = \psi_o e^{j\omega(t - \frac{x\cos\phi + y\sin\phi}{cG})} e^{-\frac{\sigma_x \cos\phi}{\varepsilon_o cG} x} e^{-\frac{\sigma_y \sin\phi}{\varepsilon_o cG} y} \tag{4a}$$

$$Z = \sqrt{\mu_o/\varepsilon_o}/G \tag{4b}$$

where Z is the wave impedance, c is the speed of light, ϕ is the angle between the wave electric field vector and the y axis, and

$$G = \sqrt{w_x \cos^2\phi + w_y \sin^2\phi} \tag{5a}$$

$$w_x = \frac{1 - j\sigma_x/\omega\varepsilon_o}{1 - j\sigma_x^*/\omega\mu_o}, \qquad w_y = \frac{1 - j\sigma_y/\omega\varepsilon_o}{1 - j\sigma_y^*/\omega\mu_o} \tag{5b}$$

Now, let each pair (σ_x, σ_x^*) and (σ_y, σ_y^*) satisfy (1). Then, w_x, w_y and G equal one at any frequency, and the wave components and the wave impedance of (4) become:

$$\psi = \psi_o e^{j\omega(t - \frac{x\cos\phi + y\sin\phi}{c})} e^{-\frac{\sigma_x \cos\phi}{\varepsilon_o c}x} e^{-\frac{\sigma_y \sin\phi}{\varepsilon_o c}y} \tag{6a}$$

$$Z = \sqrt{\mu_o/\varepsilon_o} \tag{6b}$$

Equation 6 shows that the wave in the PML medium propagates with exactly the vacuum speed of light, but decays exponentially along x and y. Equation 6 also shows that the wave impedance of the PML medium exactly equals that of vacuum regardless of the angle of propagation or frequency.

In a 2-D TE grid (x and y coordinates), Berenger proposes a normal free-space FD-TD computational zone surrounded by a PML backed by perfectly conducting (PEC) walls. At both the left and right sides of the grid ($x_{\min}$ and $x_{\max}$), each PML has σ_x and σ_x^* matched according to (1) along with $\sigma_y = \sigma_y^* = 0$ to permit reflectionless transmission across the vacuum-PML interface. At both the lower and upper sides of the grid ($y_{\min}$ and $y_{\max}$), each PML has σ_y and σ_y^* matched according to (1) along with $\sigma_x = \sigma_x^* = 0$. At the four corners of the grid where there is overlap of two PML's, all four losses are present ($\sigma_x, \sigma_x^*, \sigma_y$, and σ_y^*) and set equal to those of the adjacent PML's. Berenger proposes that the loss should increase gracefully with depth, ρ, within each PML as $\sigma(\rho) = \sigma_{\max}(\rho/\delta)^n$, where δ is the PML thickness and σ is either σ_x or σ_y. This yields a PML reflection factor of

$$R(\theta) = e^{-2\sigma_{\max}\delta\cos\theta/(n+1)\varepsilon_o c}, \tag{7}$$

which reduces to a key user-defined parameter discussed later, $R(0) = e^{-2\sigma_{\max}\delta/(n+1)\varepsilon_o c}$, the theoretical reflection coefficient at normal incidence for the PML over PEC. While $R \approx 1$ for grazing incidence, this has not been a problem in actual FD-TD simulations since such a wave is near normal on the perpendicular PML boundaries and is absorbed.

The attenuation to outgoing waves afforded by a PML medium is so rapid that standard Yee time-stepping cannot be used. The following is a suitable explicit exponentially differenced time advance [3], [5]:

$$E_y|^{n+1}_{i,j+1/2} = e^{-\sigma\Delta t/\varepsilon_o} E_y|^n_{i,j+1/2} + \frac{1}{\sigma\Delta x}(e^{-\sigma\Delta t/\varepsilon_o} - 1) \left(H_z|^{n+1/2}_{i+1/2,j+1/2} - H_z|^{n+1/2}_{i-1/2,j+1/2}\right) \tag{8}$$

III. Extension to the Full-vector Three-Dimensional Case

This section and the next represent the contributions of this letter.[1] In three-dimensions, all six Cartesian field vector components are split and the resulting PML modification of Maxwell's equations yields 12 equations, as follows:

$$\mu_o\frac{\partial H_{xy}}{\partial t} + \sigma_y^* H_{xy} = -\frac{\partial(E_{zx} + E_{zy})}{\partial y} \tag{9a}$$

$$\mu_o\frac{\partial H_{xz}}{\partial t} + \sigma_z^* H_{xz} = \frac{\partial(E_{yx} + E_{yz})}{\partial z} \tag{9b}$$

$$\mu_o\frac{\partial H_{yz}}{\partial t} + \sigma_z^* H_{yz} = -\frac{\partial(E_{xy} + E_{xz})}{\partial z} \tag{9c}$$

$$\mu_o\frac{\partial H_{yx}}{\partial t} + \sigma_x^* H_{yx} = \frac{\partial(E_{zx} + E_{zy})}{\partial x} \tag{9d}$$

$$\mu_o\frac{\partial H_{zx}}{\partial t} + \sigma_x^* H_{zx} = -\frac{\partial(E_{yx} + E_{yz})}{\partial x} \tag{9e}$$

$$\mu_o\frac{\partial H_{zy}}{\partial t} + \sigma_y^* H_{zy} = \frac{\partial(E_{xy} + E_{xz})}{\partial y} \tag{9f}$$

$$\varepsilon_o\frac{\partial E_{xy}}{\partial t} + \sigma_y E_{xy} = \frac{\partial(H_{zx} + H_{zy})}{\partial y} \tag{10a}$$

$$\varepsilon_o\frac{\partial E_{xz}}{\partial t} + \sigma_z E_{xz} = -\frac{\partial(H_{yx} + H_{yz})}{\partial z} \tag{10b}$$

$$\varepsilon_o\frac{\partial E_{yz}}{\partial t} + \sigma_z E_{yz} = \frac{\partial(H_{xy} + H_{xz})}{\partial z} \tag{10c}$$

$$\varepsilon_o\frac{\partial E_{yx}}{\partial t} + \sigma_x E_{yx} = -\frac{\partial(H_{zx} + H_{zy})}{\partial x} \tag{10d}$$

$$\varepsilon_o\frac{\partial E_{zx}}{\partial t} + \sigma_x E_{zx} = \frac{\partial(H_{yx} + H_{yz})}{\partial x} \tag{10e}$$

$$\varepsilon_o\frac{\partial E_{zy}}{\partial t} + \sigma_y E_{zy} = -\frac{\partial(H_{xy} + H_{xz})}{\partial y} \tag{10f}$$

PML matching conditions and grid structure analogous to the TE and TM cases are utilized.

IV. Numerical Experiments

We conducted numerical experiments that implemented the PML ABC in Cartesian, cubic-cell FD-TD grids, including 3-D grids, and compared its accuracy versus well-characterized Mur second-order ABC's. Our methodology was identical to that published in [6]. Cases discussed here include: 1) 2-D TE grid, vacuum region = 100×50 cells; and 2) 3-D full-vector lattice, vacuum region = $100 \times 100 \times 50$ cells.

The experiments involved exciting a pulse source centered within the vacuum region of a test grid, Ω_T. The excitation was a "smooth compact pulse" having an extremely smooth transition to zero (its first five derivatives vanishing) [6]. Ω_T was terminated by either second-order Mur or by a PML backed by PEC walls. A benchmark FD-TD solution having zero ABC artifact was obtained by running a large mesh, Ω_B, centered upon and registered with Ω_T, and having an outer boundary so remote as to be causally isolated from all points of comparison between the grids.

The error of the computed fields in Ω_T due to nonphysical reflections by the grid's imperfect ABC were obtained by subtracting the field at any point within this grid (and at any time step) from the field at the corresponding space-time point in Ω_B. The error could be measured locally, i.e, plotted versus position along a line or plane parallel to the test ABC. Or, the error could be measured globally as the sum of the squares of the error at each grid point of Ω_T.

Fig. 1 graphs the global error energy for the 2-D TE grid for both Mur and PML. The Mur ABC is standard second-order, and the PML thickness is 16 cells. At $n = 100$ time steps, the PML global error energy is about 10^{-7} that of Mur, dropping to a microscopic $10^{-12}\times$ Mur at $n = 500$.

Fig. 2 compares the local electric field error due to Mur and 16-layer PML for the 3-D FD-TD grid, as observed at $n = 100$

[1] Note added in proof: See also [7].

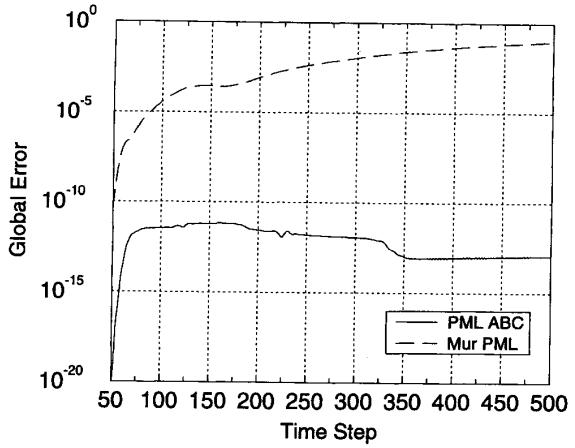

Fig. 1. Global error energy (square of the electric field error at each grid cell summed throughout the entire grid) within the 100 × 50 cell 2-D TE FD-TD grid for both the second-order Mur ABC and the 16-cell-thick PML, plotted as a function of time step number on a logarithmic vertical scale.

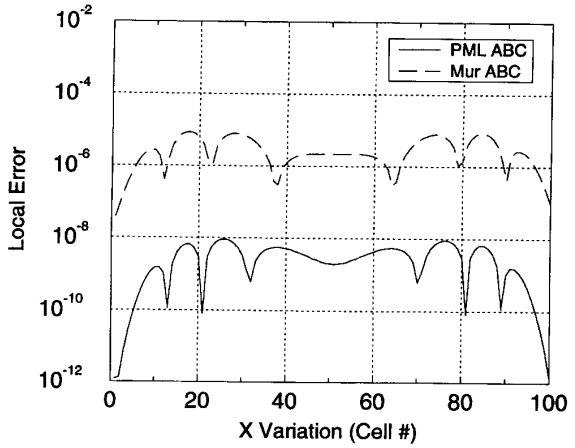

Fig. 2. Local electric field error along the x axis at the outer boundary of the 100 × 100 × 50 cell 3-D FD-TD grid for both the second-order Mur ABC and the 16-cell-thick PML, plotted on a logarithmic vertical scale (time step = 100).

time steps along the x axis at the outer boundary of Ω_T. Along this straight-line cut, the local electric field error due to PML is in the order of 10^{-3} that of Mur (i.e., about -60 dB) at a time when the ABC is being maximally excited by the outgoing wave.

In the cases of both Figs. 1 and 2, we studied the effect of varying PML thickness and the $R(0)$ parameter for a quadratically-graded loss with depth. For a fixed PML thickness, we find that reducing $R(0)$ by increasing the PML loss monotonically reduces both the local and global errors. However, this benefit levels off when $R(0)$ drops to less than 10^{-5}. We also observe a monotonic reduction of local and global error as the PML thickness increases. Here, however, a significant trade-off with the computer burden must be factored, as discussed next. Overall, the method is very insensitive to the choice of $R(0)$ and therefore losses for $R(0) < 10^{-5}$, indicating robustness.

TABLE I
TRADE-OFF OF PML ADVANTAGE OVER SECOND-ORDER MUR VERSUS COMPUTER RESOURCES FOR A 3-D BASE GRID OF 100 ×100 × 50 CELLS

ABC	Av. Local Field Error Reduction Relative to 2nd-Order Mur	Computer Resources (One CPU, Cray C-90)	If Free-Space Buffer Reduced by 5 Cells	If Free-Space Buffer Reduced by 10 Cells
Mur	1 (0 dB)	10 Mwd 6.5 sec	—	—
4-layer PML	22 (27 dB)	16 Mwd 12 sec	11 Mwd 11 sec	7 Mwd 10 sec
8-layer PML	580 (55 dB)	23 Mwd 37 sec	17 Mwd 31 sec	12 Mwd 27 sec
16-layer PML	5800 (75 dB)	43 Mwd 87 sec	33 Mwd 74 sec	25 Mwd 60 sec

Table I compares ABC effectiveness and computer burdens for second-order Mur and PML of varying thickness for the 3-D grid. Here, the arithmetic average of the absolute values of the local electric field errors over a complete planar cut through the grid at $y = 0$ and $n = 100$ is compared for Mur and PML. The last two columns indicate the potential advantage if the free-space buffer between the scatterer and the outer grid boundary were reduced by either 5 or 10 cells relative to that needed for Mur, taking advantage of the essential invisibility of the PML ABC. From these results, a PML layer 4 to 8 cells thick appears to present a good balance between ABC effectiveness and computer burden.

V. CONCLUSION

This letter verifies Berenger's strong claims for PML for 2-D FD-TD grids and extends and verifies PML for 3-D FD-TD grids. Indeed, PML is > 40 dB more accurate than second-order Mur and works just as well in 3-D as in 2-D. It should have a major impact upon the entire FD-TD modeling community, leading to new possibilities for high-accuracy simulations, especially for LO aerospace targets.

REFERENCES

[1] G. Mur, "Absorbing boundary conditions for the finite-difference approximation of the time-domain electromagnetic field equations," *IEEE Trans. Electromagnetic Compatibility*, vol. EMC-23, pp. 377–382, Nov. 1981.
[2] Z. P. Liao, H. L. Wong, B. P. Yang, and Y. F. Yuan, "A transmitting boundary for transient wave analysis," *Scientia Sinica* (series A), pp. 1063–1076, Oct. 1984.
[3] Jean-Pierre Berenger, "A perfectly matched layer for the absorption of electromagnetic waves," *J. Computational Physics*, in press.
[4] R. Holland and J. W. Williams, *IEEE Trans. Nucl. Sci.*, vol. NS-30, p. 4583, 1983.
[5] R. Holland, "Finite-difference time-domain (FDTD) analysis of magnetic diffusion," *IEEE Trans. Electromagn. Compat.*, vol. 36, pp. 32–39, Feb. 1994.
[6] T. G. Moore, J. G. Blaschak, A. Taflove and G. A. Kriegsmann, "Theory and application of radiation boundary operators," *IEEE Trans. Antenn. Propagat.*, vol. AP-36, pp. 1797–1812, Dec. 1988.
[7] J.-P. Berenger, "A perfectly matched layer for free-space simulation in finite-difference computer codes," submitted to *Annales des Telecommunications*. Also presented at EUROEM'94, Bordeaux, France, May 1994.